Polymer Chemistry

ROYAL SOCIETY OF CHEMISTRY

REVIEW

View Article Online
View Journal | View Issue

Cite this: *Polym. Chem.*, 2023, **14**, 1863

Thermo-responsive block copolymers: assembly and application

Guangran Shao,[a] Yuan Liu,[a] Rong Cao,[a] Guang Han,[b] Bing Yuan*[a] and Wangqing Zhang *[a,c]

Received 26th December 2022,
Accepted 9th March 2023

DOI: 10.1039/d2py01597h

rsc.li/polymers

Thermo-responsive block copolymers are of great interest because of their mature synthesis technology, well-defined structure, controllable molecular weight and easy implementation of their nano-assemblies in water by temperature regulation. Up to now, several previous reviews have summarized their application in biomedical fields. Thermo-responsive block copolymers also exhibit promising potential in temperature-regulated adsorption and/or separation, nanoreactors for green organic synthesis, *etc.* Herein, recent progress in their thermo-responsive assembly in water and application of five kinds of thermo-responsive block copolymers containing one or two thermo-responsive blocks beyond biomedical application is reviewed.

1. Introduction

Thermo-responsive block copolymers,[1–35] which can respond to external temperature stimuli, are block copolymers containing one or more than one thermo-responsive blocks. They have received wide attention in the fields of catalysis,[36–41] adsorption and separation,[42] wastewater treatment,[43] sensors,[44,45] imaging,[46,47] drug delivery[48] and so on. Thermo-responsive block copolymers are widely studied for three reasons. First, temperature, as the most common external stimulus in nature, is closely related to various chemical reactions and animal activities, and it provides relatively simple experimental conditions, making thermo-responsive block copolymers of great interest to researchers. Second, a wide variety of methods are available for the synthesis of thermo-responsive block copolymers, the application of "living radical polymerization", such as Nitroxide-Mediated Radical Polymerization (NMRP),[49] Reversible Addition Fragmentation Chain Transfer Polymerization (RAFT),[50,51] Atom Transfer Radical Polymerization (ATRP),[52–54] and Group Transfer Polymerization (GTP),[55,56] is well established and allows for the controlled synthesis of thermo-responsive block copolymers with well-defined structure, accurate molecular weight,

[a]*Key Laboratory of Functional Polymer Materials of the Ministry of Education, Institute of Polymer Chemistry, College of Chemistry, Nankai University, Tianjin 300071, China. E-mail: johnny.yuan@mail.nankai.edu.cn, wqzhang@nankai.edu.cn*
[b]*State Key Laboratory of Special Functional Waterproof Materials, Beijing Oriental Yuhong Waterproof Technology Co., Ltd, Beijing 100123, China*
[c]*Haihe Laboratory of Sustainable Chemical Transformations, Tianjin 300192, China*

Guangran Shao

Guangran Shao is currently a Ph.D. student at Nankai University under the supervision of Prof. Wangqing Zhang. She received a B.S. degree from the University of Jinan in 2020. Her Ph.D. studies are focused on the synthesis and application of block copolymers.

Yuan Liu

Yuan Liu is currently a Ph.D. student at Nankai University under the supervision of Prof. Wangqing Zhang. He obtained his M.S. degree in Chemical and Biological Engineering in 2019 at the China University of Petroleum (East China). His Ph.D. studies are focused on the synthesis of block copolymer nano-assemblies.

and narrow molecular weight distribution, which can facilitate the study of thermo-sensitive behavior. Finally, the condition of thermo-responsive block copolymers embodying temperature-sensitive characteristics is not easily disturbed by other stimuli. Consequently, monomers for thermo-responsive blocks can be copolymerized with other monomers to form thermo-responsive block or graft copolymers,[57–62] which can provide great convenience for study and applications.

The critical parameter for thermo-responsive block copolymers is the critical phase transition temperature, at which thermo-responsive blocks undergo phase separation. According to the performance of thermo-responsive polymers in the warming process, the critical phase transition temperature can be divided into a lower critical solution temperature (LCST) and an upper critical solution temperature (UCST). In the former case, the thermo-responsive polymers become hydrophobic from the hydrophilic state in solvents as temperature increases, while in the latter case thermo-responsive polymers become hydrophilic from the hydrophobic state. In the current literature, LCST-type thermo-responsive polymers are mostly studied, which mainly include polyacrylamides,[63–65] polyethylene oxides,[66–69] polyacrylates[70–73] and polyimidazoles,[43,74,75] which can undergo phase transition in water, and their applications in biomedical[76,77] and wastewater treatment[4,43,58] are investigated. UCST-type thermo-responsive polymers are mainly amphiphilic polyelectrolytes, such as polysulfone betaines,[78,79] poly(*N*-acryloyl glycinamide)[27,80] and ionic polypeptides.[81,82] Structures determine functionalities. In order to obtain desired block copolymers, researchers can purposefully select monomers and design block copolymers to better exploit their often-high inherent functionalities. Not only can monomers used to build block copolymers be functionalized,[9,83] but the phase transition temperature of thermo-responsive block copolymers can also be adjusted by copolymerizing with either hydrophilic or hydrophobic monomers,[84] modifying hydrophilic/hydrophobic end groups,[85] adjusting the molecular weight of block copolymers, the ratio of hydrophilic/hydrophobic monomers, the ionic strength of aqueous solution[86] and the polymer concentration.[57,59–61,87] The increase in molecular weight of hydrophobic blocks and copolymerization with hydrophobic monomers will result in a lower phase transition temperature of LCST-type block copolymers.[60,61] To obtain small sized nano-assemblies, a high concentration of block copolymers or a rapid warming process is appropriate.[16] There have been many related studies on these, so we will not go into details here.

Up to now, applications of thermo-responsive block copolymers have mostly focused on biomedical fields, such as imaging and drug delivery.[88–92] In this review, we mainly discuss their applications in other fields in conjunction with their properties, based on the structure of thermo-responsive block copolymers and their nano-assemblies. According to the composition and polymer backbone, we will summarize the self-assembly behaviors and applications of five kinds of thermo-responsive block copolymers, *i.e.*, thermo-responsive diblock copolymers containing a hydrophilic block and a thermo-responsive block, thermo-responsive diblock copolymers containing a hydrophobic block and a thermo-responsive block, doubly thermo-responsive diblock copolymers containing two thermo-responsive blocks, thermo-responsive triblock copolymers containing a hydrophilic block and two thermo-responsive blocks, and thermo-responsive triblock copolymers containing a hydrophobic block and two thermo-responsive blocks. We attempt to provide an overview to guide the design of and stimulate more applications of these thermo-responsive block copolymers.

It should be pointed out that non-linear copolymers, including grafted and/or star-shaped thermo-responsive copolymers, are also of interest and have been extensively investigated, such as poly(methyl methacrylate-*co*-hydroxylethyl methacrylate)-*g*-poly(*N*-isopropylacrylamide) amphiphilic grafted copolymers,[93] polystyrene$_n$-[poly(2-vinylpyridine)-*b*-poly(acrylic acid)-*g*-poly(*N*-isopropylacrylamide)]$_n$ heteroarm star grafted quarterpolymer,[94,95] and (cholic acid)-[poly(allyl glycidyl ether)$_n$-*b*-poly(ethylene glycol)$_m$]$_4$ star block copolymers.[96] In section 2.2, we have chosen a few typical examples to give a description of their assembly and application.

Rong Cao

Rong Cao is currently a Ph.D. student at Nankai University under the supervision of Prof. Wangqing Zhang. She obtained her M.S. degree in Material Engineering in 2020 at Tianjin University of Technology. Her Ph.D. studies are focused on the application of block polymers in membrane separation.

Guang Han

Dr Guang Han got his Ph.D. degree in polymer chemistry and physics from Nankai University with Prof. Huiqi Zhang in 2015. After that, he joined Beijing Oriental Yuhong Waterproof Technology Co., Ltd. as a senior engineer. His research interests focus on the effects of exogenous particles on the performance of waterproof materials.

2. Assembly and application of thermo-responsive block copolymers

In this section, the assembly behaviors of thermo-responsive block copolymers are summarized and their typical applications are highlighted.

2.1 Thermo-responsive diblock copolymers containing a hydrophilic block

Thermo-responsive diblock copolymers containing a hydrophilic block and a LCST-type thermo-responsive block are discussed herein. The thermo-responsive blocks can be formed by polymerization of a single monomer or copolymerization of the thermo-response originated monomer with other monomers to regulate the phase transition temperature. Generally, the LCST increases with the addition of hydrophilic comonomers and decreases with the addition of hydrophobic comonomers. Most of these block copolymers, such as poly(*N*-isopropylacrylamide)-*b*-poly(acrylic acid) (PNIPAM-*b*-PAA),[15] poly(*N*-isopropylacrylamide)-*b*-poly(ethylene glycol) (PNIPAM-*b*-PEG),[16] poly[di(ethylene glycol)ethyl ether acrylate]-*b*-poly(*N*,*N*-dimethylacrylamide) (PDEGA-*b*-PDMA)[50] and poly(ethylene glycol)-*b*-poly[(methoxy di(ethylene glycol) acrylate)-(ethoxy di(-ethylene glycol) acrylate)] [PEG-*b*-P(mDEGA-eDEGA)],[87] are dissolved in water below the LCST and then form micelles or micellar aggregates as the temperature increases above the LCST. The above diblock copolymers are summarized in Table 1.

Fig. 1 shows the phase transition behavior of such thermo-responsive diblock copolymers in water, and the typical diblock copolymer of PDEGA-*b*-PDMA,[50] in which the PDEGA block is temperature sensitive, is discussed. When the temperature is below the LCST, the hydrogen bond between the PDEGA chains and water molecules is stronger than the interaction within and/or among the PDEGA chains, the water molecules form a solvent layer around the ethoxy group through hydrogen bonding, and thus the PDEGA block is in a hydrophilic state. Since the PDMA block is hydrophilic, the PDEGA-*b*-PDMA thermo-responsive diblock copolymer is dissolved in water. The hydrogen bond interaction becomes weaker with increasing temperature. When the temperature increases above the LCST of the PDEGA block, the solvent layer of water is broken, the interaction within and/or among the PDEGA chains dominates, the PDEGA block starts to collapse and becomes insoluble in water, and the PDEGA-*b*-PDMA diblock copolymer starts to self-assemble in water to form nano-assemblies with the PDEGA block as the core and the PDMA block as the corona, which can steadily disperse in water. The transformation of the hydrophilic/hydrophobic state of the thermo-responsive PDEGA block is reversible, which can be achieved by regulating temperature below and above the LCST. When the temperature drops below the LCST, the PDEGA-*b*-PDMA diblock copolymer molecularly dissolves in water again.

The formation and dissociation of thermo-responsive diblock copolymer nano-assemblies can be reversibly switched by temperature control, and these nano-assemblies can be used for organic synthesis in water, which can reduce the use of organic solvents. Rikukawa and coworkers have undertaken systemic research in this field.[36,37] In 2019, they synthesized a thermo-responsive diblock copolymer of poly(*N*-isopropylacrylamide)-*b*-poly(sodium 4-styrenesulfonate) (PNIPAM-*b*-PSSNa) *via* RAFT polymerization.[37] The substrates, catalysts, bases used for the palladium-catalyzed Mizoroki–Heck reaction, and the PNIPAM-*b*-PSSNa diblock copolymer were added to water at room temperature and then heated. When the temperature increased above the LCST of the PNIPAM block, the PNIPAM block became hydrophobic and the diblock copolymer assembled into micelles, causing the system to become opaque. The organic compounds were more easily enriched in the hydrophobic core of the micelles compared to water; hence, the Mizoroki–Heck reaction proceeded inside the hydrophobic core of the micelles, as shown in Fig. 2. When

Bing Yuan

Dr Bing Yuan received his B.S. and M.S. degrees from Sichuan University and Lanzhou University in 2013 and 2016, respectively. He got his Ph.D. degree in polymer chemistry and physics from Nankai University with Prof. Wangqing Zhang in 2019. His current research interests include polymer self-assemblies and secondary batteries.

Wangqing Zhang

Prof. Wangqing Zhang received his B.S. and M.S. degrees from Nankai University in 1992 and 2001, respectively. He got his Ph.D. degree in polymer chemistry and physics from Nankai University with Prof. Linqin Shi in 2004. Then, he joined Nankai University in 2004 as an associate professor and became a full professor in 2010. He was awarded the National Science Foundation for Distinguished Young Scholars in 2015. His current research interests include stimuli-responsive polymers and polymeric colloids.

Table 1 Summary of thermo-responsive diblock copolymers containing a hydrophilic block

Num.	Block copolymers	Abbreviation	Ref.
1	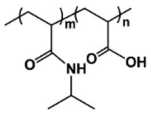	PNIPAM-*b*-PAA	15
2	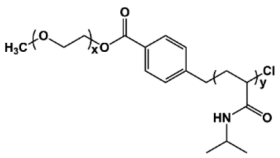	PNIPAM-*b*-PEG	16
3	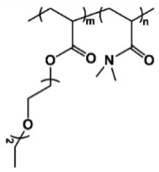	PDEGA-*b*-PDMA	50
4	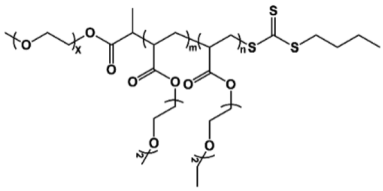	PEG-*b*-P(mDEGA-eDEGA)	83
5	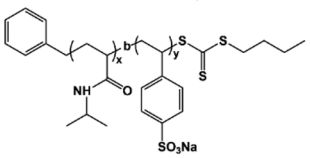	PNIPAM-*b*-PSSNa	37
6	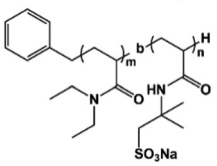	PDEAM-*b*-PAMPSNa	36
7	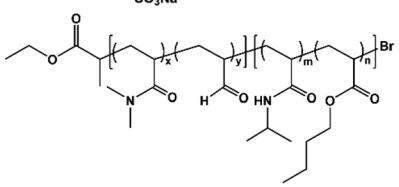	P(NIPAM-*co*-*n*BA)-*b*-P(DMA-*co*-AA)	38

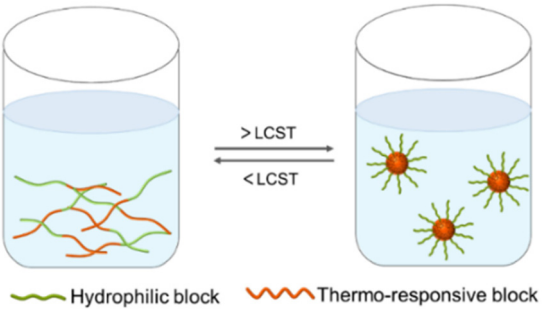

Fig. 1 Schematic phase transition of thermo-responsive diblock copolymers containing a hydrophilic block and a LCST-type thermo-responsive block.

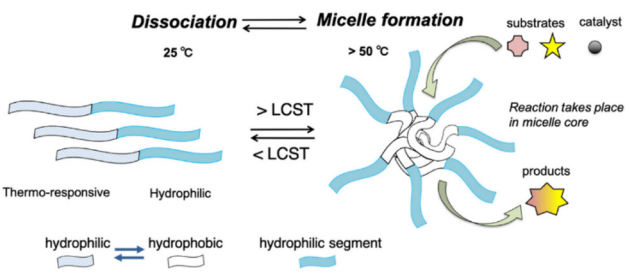

Fig. 2 Thermo-responsive micelles formed by thermo-responsive diblock copolymers for organic synthesis. Reprinted with permission from ref. 37. Copyright 2019 MDPI.

the Mizoroki–Heck reaction was completed and the system cooled to room temperature, the micelles dissociated while the products were released and the thermo-responsive diblock copolymer was re-dissolved in water. By comparing the experimental results, it was found that the product yield employing the thermo-responsive diblock copolymer micelles was as high as 99%, while the yield employing the conventional surfactant sodium dodecyl sulfate (SDS) was only 47% with the same quantity of catalyst. Besides, they also found that the thermo-responsive diblock copolymer poly(*N,N*-diethylacrylamide)-*b*-poly(sodium 2-acrylamido-methylpropane sulfonate) could act similarly to PNIPAM-*b*-PSSNa in green organic synthesis in water.[36]

In 2022, Wang's group prepared a thermo-responsive nanoreactor for phenolic compound polymerization using diblock copolymer poly(*N*-isopropylacrylamide-*co*-butyl acrylate)-*b*-poly(dimethyl acrylamide-*co*-acrylic acid) [P(NIPAM-*co*-*n*BA)-*b*-P(DMA-*co*-AA)], which shows a LCST at 37 °C in water.[38] Firstly, the synthesis of the thermo-responsive diblock copolymer was based on ATRP of DMA, *tert*-butyl acrylate (*t*BA), NIPAM, and *n*BA, yielding the diblock copolymer P(NIPAM-*co*-*n*BA)-*b*-P(DMA-*co*-*t*BA). And then hydrolysis of the *t*BA ester in the presence of trifluoroacetic acid (TFA) yielded the diblock copolymer P(NIPAM-*co*-*n*BA)-*b*-P(DMA-*co*-AA). Finally, the target horseradish peroxidase (HRP)-conjugated diblock copolymer P(NIPAM-*co*-*n*BA)-*b*-P(DMA-*co*-AA)-HRP was synthesized through a condensation reaction between the carboxylic group in the P(DMA-*co*-AA) block and the amino group in HRP. As shown in Fig. 3, when the temperature increased to 37 °C, the P(NIPAM-*co*-*n*BA) block became hydrophobic to collapse to form the core and the thermo-responsive diblock copolymer nanoreactor was formed. Enzymatic polymerization of phenolic compounds catalyzed by HRP occurred in the hydrophobic core. After the polymerization, the aqueous solution was cooled down to 22 °C, the thermo-responsive nanoreactor would be completely disassembled and the corresponding diblock copolymer P(NIPAM-*co*-*n*BA)-*b*-P(DMA-*co*-AA)-HRP became completely soluble in water, and the dissolved diblock copolymers could not catalyze the polymerization of phenolic compounds. The insoluble polyphenol could form precipitates to facilitate separation from aqueous solution. Thermo-responsive diblock copolymer nanoreactors enabled reversible formation and dissociation by ramping up/down the temperature and could be recycled for at least 10 consecutive runs with high monomer conversion and a high yield of products. Besides, the products obtained by the thermo-responsive diblock copolymer nanoreactors compared to those obtained by the conventional micellar system had higher molecular weight and better regioselectivity.

Assembly and dissociation of thermo-responsive diblock copolymers containing a hydrophilic block are temperature controlled and easily regulated with good reversibility and recyclability, which facilitate green organic synthesis in water. The phase transition temperature of the thermo-responsive block can be adjusted over a wide temperature range by copolymerizing with other monomers, which broadens the application of thermo-responsive block copolymers to a certain extent.

2.2 Thermo-responsive diblock copolymers containing a hydrophobic block

In this section, thermo-responsive diblock copolymers containing a LCST-type thermo-responsive block and a hydrophobic block are discussed. These thermo-responsive diblock copolymers include polystyrene-*b*-poly(*N*-isopropylacrylamide) (PS-*b*-PNIPAM),[17] poly(*N*-isopropylacrylamide)-*b*-poly(vinylidene fluoride) (PNIPAM-*b*-PVDF),[18] and the dendritic-linear block copolymer Den-PEtOx,[43] and they can form diblock copolymer nano-assemblies in water below the phase transition temperature of LCST. Some of these diblock copolymers are summarized in Table 2.

Herein, using the amphiphilic thermo-responsive diblock copolymer PNIPAM-*b*-PS[17] as an example, we discuss the thermo-responsive behavior of this type of thermo-responsive diblock copolymer, schematically shown in Fig. 4. When the temperature is lower than the LCST, the PNIPAM chains are in the hydrophilic state. At this point, diblock copolymer nano-assemblies with the PS block as the core and the PNIPAM block as the corona are formed and uniformly dispersed in water. When the temperature increases above the LCST of the PNIPAM block, the PNIPAM chains become insoluble and collapse to the PS core surface, leading to aggregation of the nano-assemblies and then precipitation in water. Dispersion and aggregation of the PNIPAM-*b*-PS nano-assemblies are reversible by regulating the temperature. When the temperature decreases below the LCST, the PNIPAM-*b*-PS nano-assemblies are uniformly dispersed into water again.

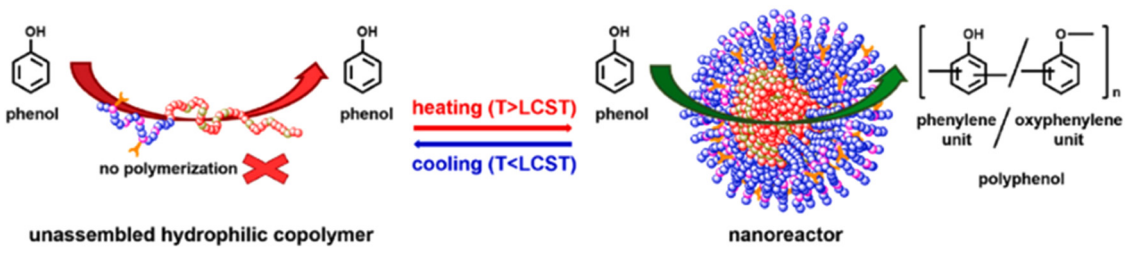

Fig. 3 Enzymatic polymerization of phenolic compounds catalyzed by HRP within nanoreactors of thermo-responsive diblock copolymer. Reprinted with permission from ref. 38. Copyright 2022 The Royal Society of Chemistry.

Table 2 Summary of thermo-responsive diblock copolymers containing a hydrophobic block

Num.	Block copolymers	Abbreviation	Ref.
1	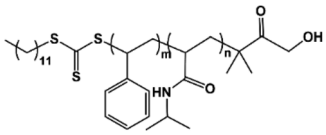	PS-*b*-PNIPAM	17
2	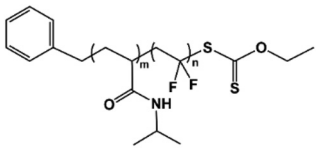	PNIPAM-*b*-PVDF	18
3	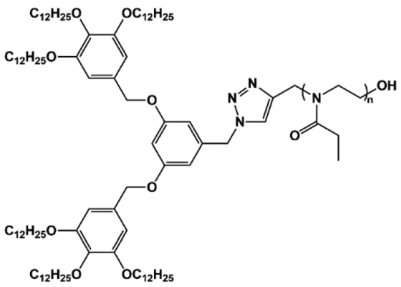	Den-PEtOx	43
4	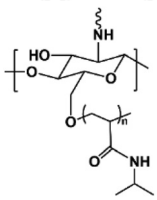	MCM-PNIPAM	57
5	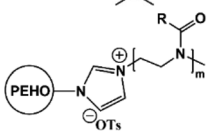	PEHO-IL-Pox	74

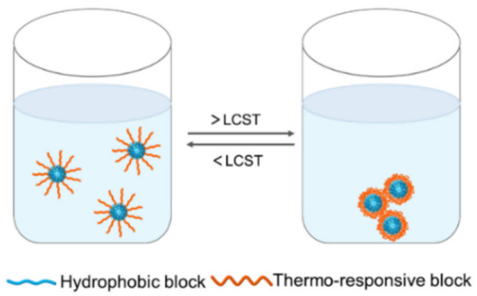

Fig. 4 Schematic phase transition of thermo-responsive diblock copolymers containing a hydrophobic block.

In 2019, Jang and coworkers prepared the thermo-responsive dendritic-linear block copolymer Den-PEtOx,[43] which showed a LCST at 62.4 °C in water, for the purification of dye-contaminated water. A schematic diagram of the purification process is shown in Fig. 5A. Firstly, PEtOx was obtained *via* cationic ring-opening polymerization of 2-ethyl-2-oxazoline (EtOx), and then post-modified with the azide group of an alkyl-bearing aryl ether dendritic wedge (Den) to obtain the amphiphilic thermo-responsive block copolymer Den-PEtOx. The diblock copolymer Den-PEtOx was assembled into micelles in an acidic aqueous solution of Rose Bengal (RB) at room temperature, and then RB entered the core of the micelles due to the π–π stacking and hydrophobic interaction between RB and Den. When the temperature increased above the LCST of the PEtOx block, the Den-PEtOx micelles with encapsulated RB formed insoluble aggregates, which could be removed by filtering. The color of the aqueous solution changed from red to colourless transparent and more than 99% of RB was removed, as shown in Fig. 5B. This work provides an innovative method for dye removal from aqueous solution using thermo-responsive block copolymers. In the same year of 2019, similar work was undertaken by Marcus and coworkers. (Magnetic chitosan microspheres)-poly(*N*-isopropylacrylamide) (MCM-PNIPAM) was synthesized by graft polymerization of NIPAM on the surface of magnetic chitosan microspheres (MCM) to be used in the treatment of oily water.[58] Below the phase transition temperature, the microspheres grafted with PNIPAM chains were uniformly dispersed in the oily water. When the temperature increased above the LCST, the grafted PNIPAM chains became oleophilic rather

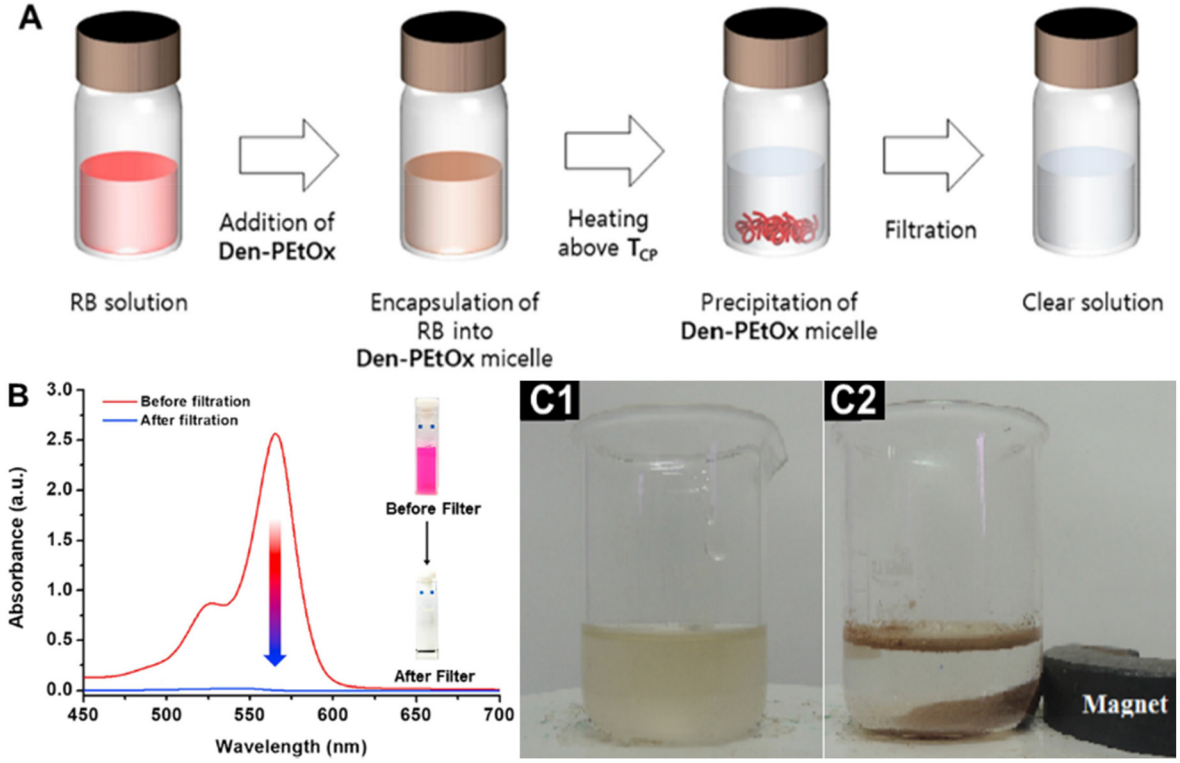

Fig. 5 (A) Schematic representation of dye-containing water purification using the thermo-responsive dendritic-linear block copolymer Den-PEtOx. (B) UV-vis absorption spectral changes of RB encapsulated in Den-PEtOx before heating (red line) and after filtration above the LCST (blue line). (C1) Images of the synthetic oily water. (C2) Images of oily water containing MCM-PNIPAM after introducing a magnetic field. (A and B) Reprinted with permission from ref. 43. Copyright 2019 Elsevier. (C1 and C2) Reprinted with permission from ref. 58. Copyright 2019 Elsevier.

than hydrophilic. At this time, the free oil droplets would be bound in the collapsed corona of PNIPAM and precipitated together. The oil-absorbed microspheres grafted with PNIPAM could be efficiently removed from water by introducing an external magnetic field, as shown in Fig. 5C1 and C2. The method to treat oil-contaminated water developed from this work showed that MCM-PNIPAM, at a particle concentration of 2% w/w, was effective in reducing oil, with oil-removal percentages higher than 97% for water containing around 500 ppm of organic phase.

Amphiphilic diblock copolymers with a thermo-responsive hydrophilic block can be used as molecular shuttles between aqueous and organic phases. Mülhaupt and coworkers prepared such molecular shuttles by grafting LCST-type thermo-responsive polyoxazolines onto hyperbranched poly(3-ethyl-3-hydroxymethyloxetane) (PEHO) ionic liquids, namely, PEHO-IL-PEtOx and PEHO-IL-P*n*PrOx.[75] As shown in Fig. 6, at 0 °C, due to electrostatic interaction, PEHO-IL-P*n*PrOx captured palladium complexes containing bis(*p*-sulfonatophenyl) phenylphosphine as ligand uniformly dispersed in aqueous solution, which could catalyze organic reactions. When heated to 70 °C, the polarity of the P*n*PrOx block decreased and it became insoluble in water, thus migrating into the ethyl acetate phase. When the temperature decreased to 0 °C, PEHO-IL-P*n*PrOx with the palladium complexes returned to water from the ethyl acetate phase. This process was repeated

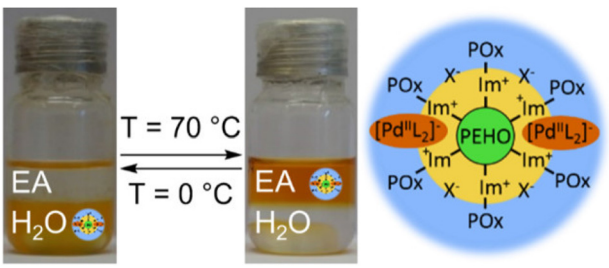

Fig. 6 PEHO-IL-P*n*PrOx as a thermo-responsive shuttle for an anionic water-soluble Pd-phosphine complex in the ethyl acetate/water two-phase system. Reprinted with permission from ref. 75. Copyright 2019 American Chemical Society.

several times without impairing shuttling. This method improves the efficiency of inorganic catalysts for organic reactions. In another study, in octane/water, thermo-responsive hairy particles, such as poly[methoxytri(ethylene glycol) methacrylate] grafted on a crosslinked poly(acrylic acid) core, were used as carriers for palladium nanoparticles, which catalyzed hydrogenation and were easily recycled.[40] Similar studies have been done in recent years, and readers can refer to the references.[39,97–100]

There is another interesting study reported by Kamperman and coworkers in 2017.[17] They presented reversible thermo-

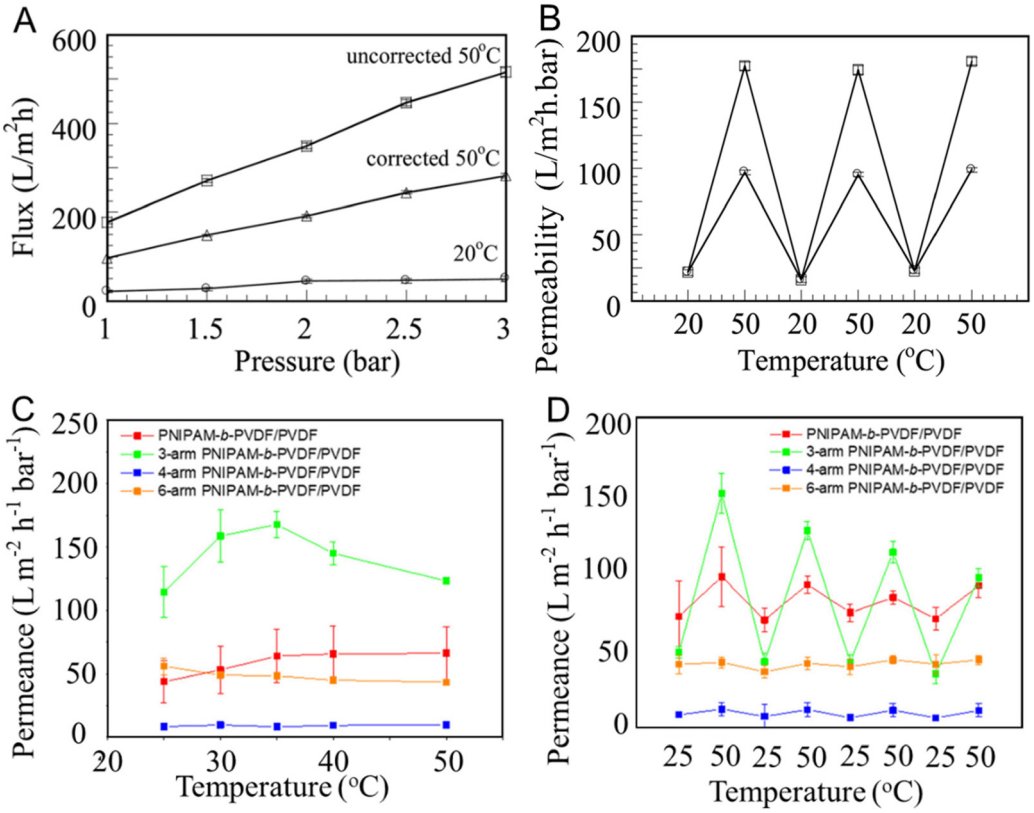

Fig. 7 (A) Flux measurements of the PS-*b*-PNIPAM membrane, (B) reversibility of the thermo-responsive behavior of the PS-*b*-PNIPAM membrane showing tunable permeability during 25–50 °C heating–cooling cycling, (C) temperature-dependent water permeance of the PNIPAM-*b*-PVDF membrane, and (D) tunable water permeance of the thermo-responsive PNIPAM-*b*-PVDF membrane during 25–50 °C heating–cooling cycling. (A and B) Reprinted with permission from ref. 17. Copyright 2017 Royal Society of Chemistry. (C and D) Reprinted with permission from ref. 18. Copyright 2021 American Chemical Society.

responsive nanoporous membranes fabricated from the PS-*b*-PNIPAM diblock copolymer obtained by RAFT polymerization. When the temperature increased from 26 to 38 °C, the water permeability increased by nearly 400%, as shown in Fig. 7A. These results demonstrated that the thermo-responsive permeability of the membrane was the result of the collapsing PNIPAM chains at temperatures above the LCST. When the temperature was below the LCST, the dissolved state of PNIPAM chains covered the nanopore surface of the membrane, resulting in lower membrane permeability. Whereas, as the temperature increased above the LCST, the PNIPAM chains collapsed and the nanopores were completely exposed, leading to a significant increase in permeability. The change in permeability was found to be reversible with temperature switching between 20 and 50 °C, indicating that the thermo-responsive permeability of the membrane was fully reversible, as shown in Fig. 7B, which provided the prospect for further development of advanced easy-to-clean membrane applications. In 2021, similar results were demonstrated by Nunes' group.[18] The membranes of the thermo-responsive PNIPAM-*b*-PVDF diblock copolymer exhibited reversible water permeation in the case of heating–cooling between 25 and 50 °C, as shown in Fig. 7C and D.

Thermo-responsive diblock copolymers containing a hydrophobic block are the most widely investigated, and their reversible phase transition provides great convenience for separation and recovery. In addition, the introduction of thermo-responsive block copolymers into adsorption and separation materials, and the dissolution and collapse of thermo-responsive blocks provide new ideas for regulating the permeability of separation membranes.

2.3 Doubly thermo-responsive diblock copolymers

Herein, doubly thermo-responsive diblock copolymers are composed of two thermo-responsive blocks with different phase transition temperatures. One is composed of two blocks with different LCSTs, such as poly(*N*-isopropylacrylamide)-*b*-poly(dimethylaminoethyl methacrylate) (PNIPAM-*b*-PDMAEMA),[12] poly(*N*-acryloylsarcosine methyl ester)-*b*-poly(*N*-isopropylacrylamide) (PNASME-*b*-PNIPAM)[20] and poly(diethylene glycol monomethyl ether methacrylate)-*b*-poly[poly(ethylene glycol) methyl ether methacrylate] (PO_2-*b*-PO_{300}).[45] The other is made up of a non-ionic hydrophilic block with a LCST and a zwitterionic block with an UCST, such as poly(sulfobetaine methacrylate)-*b*-poly(*N*-isopropylmethacrylamide) (PSBMA-*b*-PNIPMAM),[21] polysulfobetaine-*b*-poly(*N*-isopropyl-

methacrylamide) (PSPP-*b*-PNIPMAM),[22] polysulfobetaine-*b*-poly(*N*-isopropylacrylamide) (PSPP-*b*-PNIPAM)[25] and poly(dimethylaminoethyl methacrylate)-*b*-poly(sulfobetaine methacrylate) (PDMAEMA-*b*-PSBMA).[101] All the above diblock copolymers are listed in Table 3. Interestingly, the solvation state of the doubly thermo-responsive diblock copolymers bearing a non-ionic hydrophilic block and a zwitterionic block can be inverted in aqueous solution, leading to the core- and corona-forming blocks being inverted.

The self-assembly of doubly thermo-responsive diblock copolymers with two different LCSTs in aqueous solution is schematically shown in Fig. 8A. For example, for the PNASME-*b*-PNIPAM diblock copolymer,[20] when the temperature increases above the LCST of the PNIPAM block, the diblock copolymer undergoes self-assembly to form micelles, which consist of a core of the insoluble PNIPAM block surrounded by a corona of the solvated PNASME block. When the temperature continues to increase above the phase transition temperature

Table 3 Summary of doubly thermo-responsive diblock copolymers

Num.	Block copolymers	Abbreviation	Ref.
1	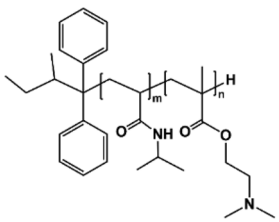	PNIPAM-*b*-PDMAEMA	12
2	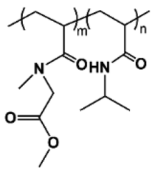	PNASME-*b*-PNIPAM	20
3	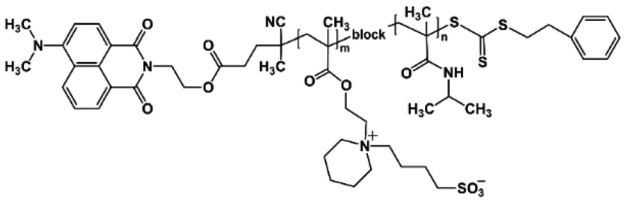	PSBMA-*b*-PNIPMAM	21
4	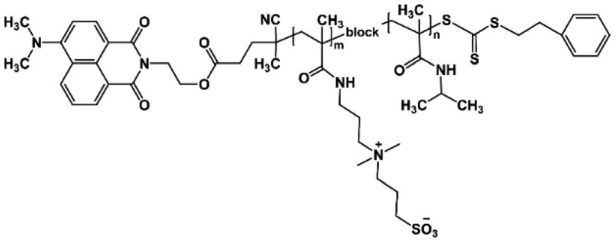	PSPP-*b*-PNIPMAM	22
5	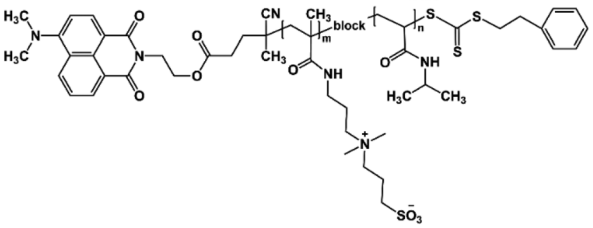	PSPP-*b*-PNIPAM	25
6	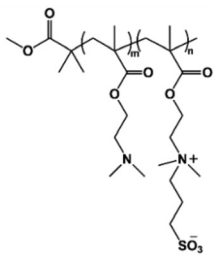	PDMAEMA-*b*-PSBMA	97

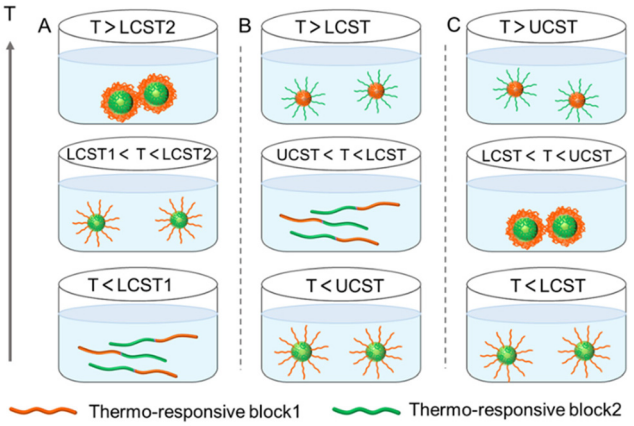

Fig. 8 Schematic phase transition of doubly thermo-responsive diblock copolymers: (A) with two different LCSTs, (B) with a lower UCST and a higher LCST, and (C) with a lower LCST and a higher UCST.

of the PNASME block, the PNASME block becomes insoluble and is then deposited onto the surface of the PNIPAM core. When the temperature gradually cools down to room temperature, the two blocks dissolve in water again one after the other. The self-assembly behavior of doubly thermo-responsive diblock copolymers containing a zwitterionic block in aqueous solution is also dependent on the UCST of the zwitterionic block and the LCST of the non-ionic block. For example, the diblock copolymer PSPP-*b*-PNIPMAM combines the upper and lower critical solution temperatures of each block in aqueous solution,[22] where the UCST of the PSPP block is lower than the LCST of the PNIPMAM block. When the temperature is lower than the UCST, the PSPP block is hydrophobic and the PNIPMAM block is in the dissolved state, the diblock copolymer assembles into micelles with the PSPP block as the core and the PNIPMAM block as the corona. When the temperature is between UCST and LCST, both the PSPP block and the PNIPMAM block are in the dissolved state, and therefore the diblock copolymer PSPP-*b*-PNIPMAM is molecularly soluble in water. When the temperature is higher than the LCST, the PSPP block is dissolved in water and the PNIPMAM block becomes hydrophobic, and PSPP-*b*-PNIPMAM forms micelles with the PNIPMAM block as the core and the PSPP block as the corona, where the core- and corona-forming blocks are inverted, as shown in Fig. 8B. However, if the UCST is higher than the LCST, diblock copolymers containing a zwitterionic block exhibit different phase transitions, as shown in Fig. 8C. When the temperature is lower than the LCST of the non-ionic block, the zwitterionic block is hydrophobic and the non-ionic block is in the dissolved state. Micelles with the zwitterionic block as the core and the non-ionic block as the corona form at this temperature. When the temperature is between the LCST and the UCST, both the zwitterionic block and the non-ionic block are hydrophobic. When the temperature is higher than the UCST, the zwitterionic block becomes hydrophilic and the non-ionic block is in a hydrophobic state, forming micelles with the non-ionic block as the core and the zwitterionic block as the corona. In these transformations, the roles of hydrophilic block and hydrophobic block are switched, and the micellar structure turns inside-out. For this self-assembly, the term "schizophrenic" had been coined to describe this transformation.

In 2022, Zhong *et al.*, prepared thin films of the thermo-responsive PO_2-*b*-PO_{300} diblock copolymer showing two different LCSTs.[45] The phase transition temperatures of the PO_2 block and the PO_{300} block are 25 °C and 60 °C, respectively. The effect of different cooling processes (one-step: 60 to 20 °C and two-step: 60 to 40 °C and then to 20 °C) on film swelling behavior was investigated by *in situ* neutron reflectivity (NR) and two different response processes are shown in Fig. 9. After the one-step stimulus (rapid decrease in temperature from 60 to 20 °C), the film directly switched from collapsed to fully swollen state. While the film presented a different swelling behavior when the thermal stimulus was separated into two steps (first decrease from 60 to 40 °C and then to 20 °C). The film switched firstly from collapsed to semi-swollen state caused by the swollen PO_{300} block after the first step of the thermal stimulus (60 to 40 °C) and then to fully swollen state induced by the swollen PO_2 block after the second step (40 to 20 °C). However, the final states of the swollen PO_2-*b*-PO_{300} film were basically identical irrespective of the applied thermal stimulus. Thus, the final state of the thermo-responsive diblock copolymer film was not affected by the external thermal stimuli, which is beneficial for the design and preparation of sensors or switches based on thermo-responsive block copolymer film.

Most of the studies on doubly thermo-responsive diblock copolymers so far have focused on the effect of external stimuli (*e.g.*, temperature, low molar mass salt) on their self-assembly in aqueous solution, and less on their applications. However, we believe that the suitable selection of monomers can confer the advantages of multiple temperature sensitivities to doubly thermo-responsive block copolymers, which can potentially be made into various membrane materials or temperature sensors to meet different needs.

2.4 Thermo-responsive triblock copolymers containing a hydrophilic block

Herein, these thermo-responsive triblock copolymers contain a hydrophilic block and two thermo-responsive blocks. According to the block components, they can be divided into two categories: namely, ABC-type doubly thermo-responsive triblock copolymers and ABA-type thermo-responsive triblock copolymers. The ABC-type doubly thermo-responsive triblock copolymers have two different thermo-responsive blocks, such as poly(ethylene oxide)-*b*-poly(*N*-acryloylglycinamide)-*b*-poly(*N*-isopropylacrylamide) (PEO-*b*-PNAGA-*b*-PNIPAM),[27] poly(propylene oxide)-*b*-poly(2-methacryloyloxyethyl phosphorylcholine)-*b*-poly(*N*-isopropylacrylamide) (PPO-*b*-PMPC-*b*-PNIPAM)[28] and poly(ethylene-*alt*-propylene)-*b*-poly(ethylene oxide)-*b*-poly(*N*-isopropylacrylamide-*co*-acrylic acid) [PEP-*b*-PEO-*b*-P(NIPAM-*co*-AA)].[59] While the ABA-type thermo-responsive triblock copolymers have the same thermo-responsive block, such as poly(*N*-

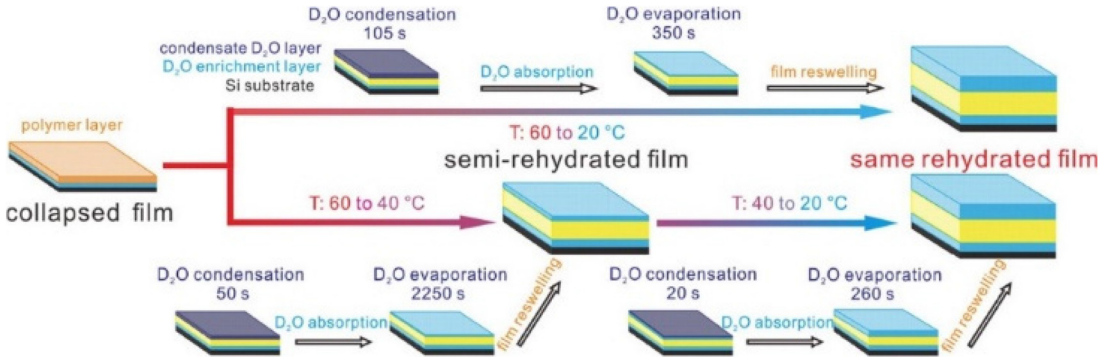

Fig. 9 Schematic diagram of the film swelling process for two different thermal stimulation processes. Reprinted with permission from ref. 45. Copyright 2022 American Chemical Society.

isopropylacrylamide)-*b*-poly(dimethylacrylamide)-*b*-poly(*N*-isopropylacrylamide) (PNIPAM-*b*-PDMA-*b*-PNIPAM),[30] poly[ethoxytri(ethylene glycol) acrylate-*co*-*o*-nitrobenzyl acrylate]-*b*-poly(ethylene oxide)-*b*-poly[ethoxytri(ethylene glycol) acrylate-*co*-*o*-nitrobenzyl acrylate] [P(TEGEA-*co*-NBA)-*b*-PEO-*b*-P(TEGEA-*co*-NBA)][53] and poly(2-*n*-propyl-2-oxazoline)-*b*-poly(2-ethyl-2-oxazoline)-*b*-poly(2-*n*-propyl-2-oxazoline) (P*n*PrOx-*b*-PEtOx-*b*-P*n*PrOx).[74] Some of the triblock copolymers are listed in Table 4.

The ABA-type and ABC-type thermo-responsive triblock copolymers show different assembly behaviors in aqueous solution during the warming process. ABC-type doubly thermo-responsive triblock copolymers,[61] where the A-block and C-block are two different thermo-responsive blocks, have two different phase transitions during temperature ramp-up. Since the two thermo-responsive blocks are separated by the hydrophilic B-block, two different hydrophobic cores connected by the hydrophilic B-block form during the warming process. When the temperature increases above the LCST of the A-block, the ABC-type doubly thermo-responsive triblock copolymer forms micelles with the A-block as core and the B-block and C-block as the corona; when the temperature continues to increase above the LCST of the C-block, the triblock copolymer forms a polymer network with the hydrophobic cores of the A-block and C-block as the crosslinking point or flower-like micelles dependent on polymer concentration, as shown in Fig. 10A. When the temperature decreases below the LCST, the triblock copolymer will be dissolved again in aqueous solution. ABA-type thermo-responsive triblock copolymers have two thermo-responsive blocks of A,[29] and since the two blocks are the same, there is just one phase transition during the warming process. As shown in Fig. 10B, when the temperature increases above the LCST of the A-block, the A-block becomes hydrophobic while the B-block is in a dissolved state, at which time flower-like micelles form with the A-block as the core and the B-block as the corona. When the concentration of polymer solution is high, crosslinked structures also form among micelles. A series of studies have been done by Tsitsilianis' group to study this dynamic crosslinking network.[102–104] In 2018, they prepared injectable hydrogels with triblock copolymers poly[(triethylene glycol methyl ether methacrylate)-*co*-(*n*-butyl methacrylate)]-*b*-poly(dimethylaminoethyl methacrylate)-*b*-poly[(triethylene glycol methyl ether methacrylate)-*co*-(*n*-butyl methacrylate)] [P(TEGMA-*co*-*n*BuMA)-*b*-PDMAEMA-*b*-P(TEGMA-*co*-*n*BuMA)].[103] The triblock copolymer solution was a viscoelastic complex fluid at low temperature and could be used for injection. During the warming process, the thermo-responsive block P(TEGMA-*co*-*n*BuMA) became insoluble in water and the chain segments were frozen to form a hydrophobic core, leading to a crosslinked structure, or so-called hydrogel.

Up to now, the applications of thermo-responsive triblock copolymers containing a hydrophilic block have been very rare. Compared with others containing thermo-responsive blocks, their assembly behavior is more influenced by the triblock copolymer concentration, and there is a possibility of forming a reversible crosslinked network structure or so-called hydrogel during the assembly process. The switch from crosslinking to decrosslinking can be achieved by adjusting the temperature. Due to the substantial improvement in mechanical properties of the dynamic crosslinking networks, their application in suspensions, coatings and cosmetics is expected.

2.5 Thermo-responsive triblock copolymers containing a hydrophobic block

In this section, triblock copolymers composed of a hydrophobic block and two thermo-responsive blocks are reviewed. Depending on whether the thermo-responsive block components are the same or not, the thermo-responsive triblock copolymers are divided into ABC-type doubly thermo-responsive triblock copolymers and ABA-type thermo-responsive triblock copolymers. For example, poly[poly(ethylene glycol) methyl ether vinylphenyl]-*b*-poly(*N*-isopropylacrylamide)-*b*-polystyrene [P(mPEGV)-*b*-PNIPAM-*b*-PS],[31] poly[2-(2-methoxyethoxy)ethyl methacrylate]-*b*-poly[oligo(ethylene glycol) methyl ether methacrylate]-*b*-poly[9-(4-vinylbenzyl)-9H-carbazole] ($PMEO_2MA$-*b*-$POEGMA_{8-9}$-*b*-PVBK)[32] and poly(*N*-isopropylacrylamide)-*b*-poly(dimethylaminoethyl methacrylate)-*b*-polystyrene (PNIPAM-*b*-PDMAEMA-*b*-PS)[33] belong to the ABC-

Table 4 Summary of thermo-responsive triblock copolymers containing a hydrophilic block

Num.	Block copolymers	Abbreviation	Ref.
1	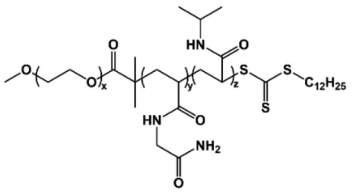	PEO-*b*-PNAGA-*b*-PNIPAM	27
2	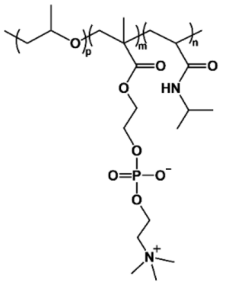	PPO-*b*-PMPC-*b*-PNIPAM	28
3	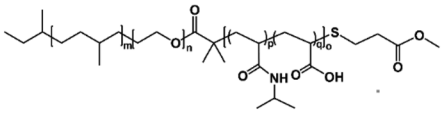	PEP-*b*-PEO-*b*-P(NIPAM-*co*-AA)	59
4	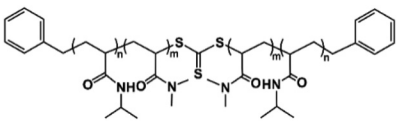	PNIPAM-*b*-PDMA-*b*-PNIPAM	30
5	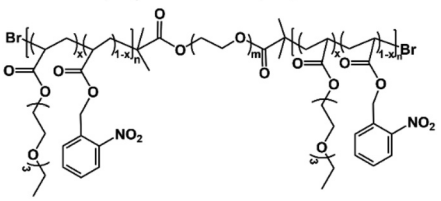	P(TEGEA-*co*-NBA)-*b*-PEO-*b*-P(TEGEA-*co*-NBA)	53
6	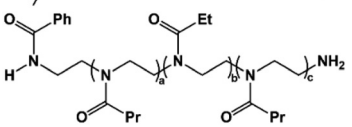	P*n*PrOx-*b*-PEtOx-*b*-P*n*PrOx	74
7	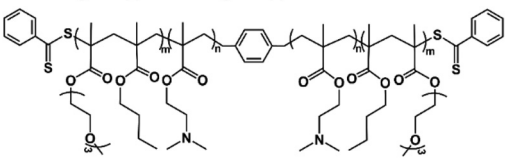	P(TEGMA-*co*-*n*BuMA)-*b*-PDMAEMA-*b*-P(TEGMA-*co*-*n*BuMA)	103

type doubly thermo-responsive triblock copolymers. Some typical ABA-type thermo-responsive triblock copolymers include poly(ethylene glycol methyl ether methacrylate)-*b*-polystyrene-*b*-poly(ethylene glycol methyl ether methacrylate) (PMENMA-*b*-PS-*b*-PMENMA),[34] poly(*N*-isopropylacrylamide)-*b*-poly(3-methacryloxypropyltrimethoxysilane)-*b*-poly(*N*-isopropylacrylamide) (PNIPAM-*b*-PMEMO-*b*-PNIPAM),[35] poly[(*N*-isopropylacrylamide)-*co*-(dimethylacrylamide)]-*b*-poly(L-lactide)-*b*-poly[(*N*-isopropylacrylamide)-*co*-(dimethylacrylamide)] [P(NIPAM-*co*-DMA)-*b*-PLLA-*b*-P(NIPAM-*co*-DMA)],[60] poly[oligo(ethylene glycol) methyl ether methacrylate]-*b*-polydimethylsiloxane-*b*-poly[oligo(ethylene glycol) methyl ether methacrylate] (POEGMA-*b*-PDMS-*b*-POEGMA),[67] and poly[oligo(ethylene glycol) methyl ether methacrylate]-*b*-poly(4-vinyl pyridine)-*b*-poly[oligo(ethylene glycol) methyl ether methacrylate] (POEGMA-*b*-P4VP-*b*-POEGMA).[68] Some of these triblock copolymers are summarized in Table 5.

ABA-type thermo-responsive triblock copolymers containing a hydrophobic block, *e.g.*, POEGMA-*b*-P4VP-*b*-POEGMA,[68] form micelles with a core–shell structure in aqueous solution below the LCST of the POEGMA block, and their phase transition behaviors are similar to those of thermo-responsive diblock copolymers containing a hydrophobic block. As shown in Fig. 11A, as the temperature of the aqueous solution increases above the LCST of the POEGMA block, the POEGMA block dehydrates and collapses to the surface of the P4VP core, and

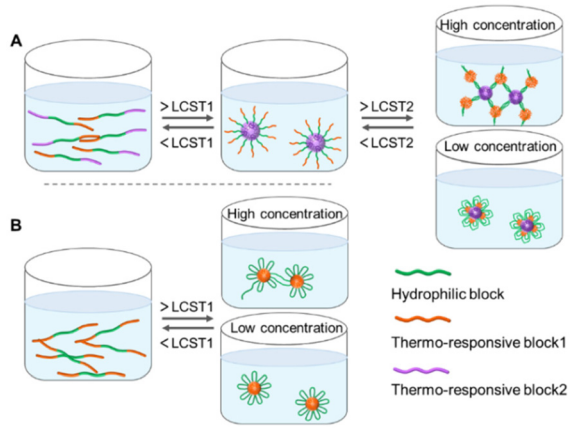

Fig. 10 Schematic diagram of the phase transition of thermo-responsive triblock copolymers containing a hydrophilic block: (A) ABC-type, (B) ABA-type.

nanoparticles with P4VP as the core and POEGMA as the shell form and then aggregate and precipitate in solvent. Since the ABC-type doubly thermo-responsive triblock copolymers have two different LCSTs, their phase transition process in aqueous solutions is different from the ABA-type mentioned above. It is worth noting that the location of the hydrophobic block can affect the self-assembly of ABC-type doubly thermo-responsive triblock copolymers. As shown in Fig. 11B, when the hydrophobic block is the middle block, thermo-responsive ABC triblock copolymers, *e.g.*, PDMAEMA-*b*-PS-*b*-PNIPAM,[105] form core–corona nanoparticles. When the temperature increases above the first LCST, the thermo-responsive block with low LCST becomes dehydrated to deposit on the hydrophobic core, and the corona–core nanoparticles convert into corona–shell–core ones; when the temperature further increases above the second LCST, the thermo-responsive block with high LCST becomes dehydrated to form shell–shell–core nanoparticles. When the hydrophobic block is the terminal block, the ABC-type doubly thermo-responsive triblock copolymers exhibit different phase transitions depending on the sequence of the two thermo-responsive blocks during the warming process. As shown in Fig. 11C, for thermo-responsive ABC triblock copolymers in which the A-block has a high LCST and the B-block has a low LCST, *e.g.*, PDMAEMA-*b*-PNIPAM-*b*-PS,[33] their phase transition behaviour during the warming process is similar to that containing a middle hydrophobic block shown in Fig. 11B. In the case of the ABC triblock copolymer containing an A-block with a low LCST and a B-block with a high LCST, as shown in Fig. 11D, *e.g.*, PNIPAM-*b*-PDMAEMA-*b*-PS,[33] their self-assembly behavior is influenced by the polymer concentration. That is, flower-like micelles or crosslinked assemblies are formed during the warming process.

In 2008, Kang and coworkers prepared thermo-responsive membranes with poly(*N*-isopropylacrylamide)-*b*-polycaprolactone-*b*-poly(*N*-isopropylacrylamide) (PNIPAM-*b*-PCL-*b*-PNIPAM),[54] called PCL-PNP membrane. The thermo-responsive characteristics of the PCL-PNP membrane were illustrated by glucose transport across the membranes. The PNIPAM-*b*-PCL-*b*-PNIPAM thermo-responsive triblock copolymers were prepared *via* ATRP, and were then cast to form microporous PCL-PNP membranes by phase inversion in an aqueous medium. A glucose permeation experiment, as shown in Fig. 12A, demonstrated the membrane thermal response. They examined the glucose transport rate using the PCL-PNP membranes at 20 and 37 °C, below and above the LCST, respectively. The results showed that the glucose transport rate of the PCL-PNP membranes at 37 °C above the LCST was higher than those at 20 °C below the LCST, as shown in Fig. 12B. This is caused by the hydrophilic-to-hydrophobic transition of the thermo-responsive PNIPAM block. At 20 °C below the LCST, the thermo-responsive PNIPAM block was hydrophilic and the PNIPAM chains were fully extended in the solution covering the surface of the membrane to hinder glucose diffusion. As the temperature increased to 37 °C above the LCST, the PNIPAM chains collapsed and the pores on the membrane surface were exposed, which caused less hindrance to the glucose transport across the membrane, and consequently the rate of glucose transport increased. The pore size of the PCL-PNP membrane can also be tuned by adjusting the length of the PNIPAM block to regulate the glucose transport rate. In 2016, Yokoyama's group also made thermo-responsive membranes composed of a mesoporous layer of PMENMA-*b*-PS-*b*-PMENMA and a supporting layer of polyvinylidene fluoride (PVDF).[34] They demonstrated temperature-responsive sieving of gold nanoparticles through the composite membranes, in which the mesopore size increased with increasing temperature (Fig. 12C), and therefore the concentration of gold nanoparticles in the filtrate gradually increased during the warming process, as shown in Fig. 12D.

Similar to thermo-responsive diblock copolymers containing a hydrophobic block, thermo-responsive triblock copolymers containing a hydrophobic block can assemble into micelles in aqueous solution, and the core composed of the hydrophobic block can encapsulate dyes or drugs dispersed in aqueous solution; hence, they are also used for drug delivery and separation of dyes in wastewater. In 2011, Yu and coworkers prepared poly(*N*-isopropylacrylamide)-*b*-poly(*n*-octadecylacrylate)-*b*-poly(*N*-isopropylacrylamide) (PNIPAM-*b*-PODA-*b*-PNIPAM) *via* RAFT polymerization.[51] The PNIPAM-*b*-PODA-*b*-PNIPAM micelles showed high drug loading efficiency up to 14.68%, indicating their potential as drug carriers.

Thermo-responsive triblock copolymers composed of a hydrophobic block and two thermo-responsive blocks can form micelles in aqueous solution, and the self-assembled micelles can be used not only for encapsulating drugs or dyes, but also as nanoreactors for performing organic reactions in aqueous solution, as emulsifiers for easy control of emulsification and demulsification, *etc*. In addition, the triblock copolymers can be used to prepare thermo-responsive membranes, which can regulate the transport rate across the membrane by tuning the pore size through the temperature-dependent stretching or collapse of the thermo-responsive blocks.

Table 5 Summary of thermo-responsive triblock copolymers containing a hydrophobic block

Num.	Block copolymers	Abbreviation	Ref.
1	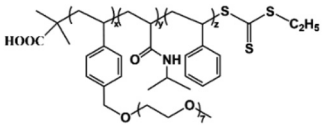	P(mPEGV)-*b*-PNIPAM-*b*-PS	31
2	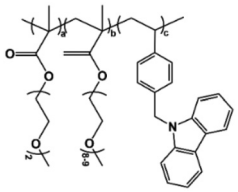	$PMEO_2MA$-*b*-$POEGMA_{8-9}$-*b*-PVBK	32
3	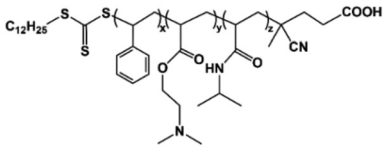	PNIPAM-*b*-PDMAEMA-*b*-PS	33
4	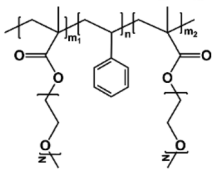	PMENMA-*b*-PS-*b*-PMENMA	34
5	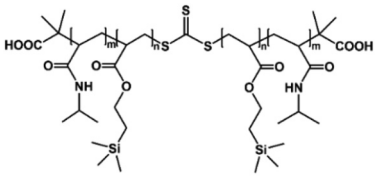	PNIPAM-*b*-PMEMO-*b*-PNIPAM	35
6	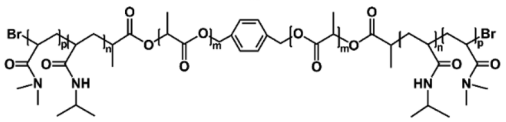	[P(NIPAM-*co*-DMAM)-*b*-PLLA-*b*-P(NIPAM-*co*-DMAM)]	60
7	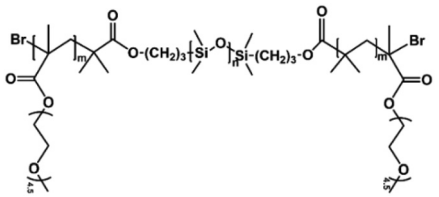	POEGMA-*b*-PDMS-*b*-POEGMA	67
8	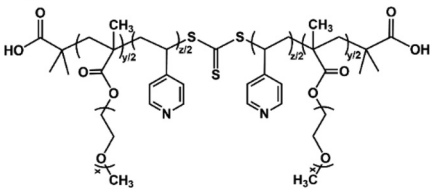	POEGMA-*b*-P4VP-*b*-POEGMA	68
9	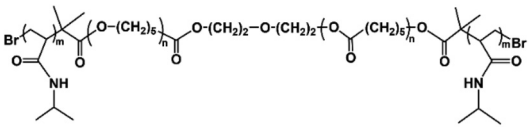	PNIPAM-*b*-PCL-*b*-PNIPAM	54
10	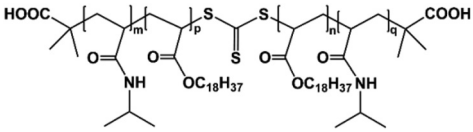	PNIPAM-*b*-PODA-*b*-PNIPAM	51

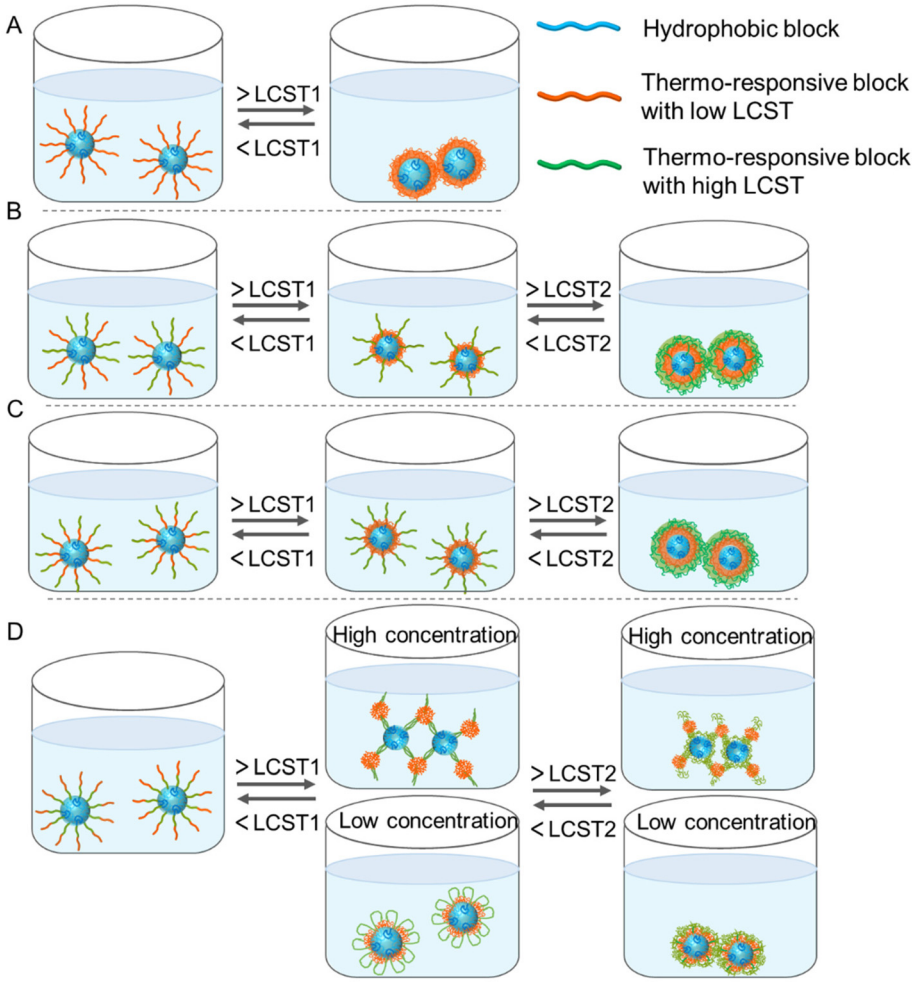

Fig. 11 Schematic phase transition of thermo-responsive triblock copolymers containing a hydrophobic block: (A) ABA-type; (B) ABC-type: with a hydrophobic B-block; (C) ABC-type: A-block with a high LCST and B-block with a low LCST and (D) ABC-type: A-block with a low LCST and B-block with a high LCST.

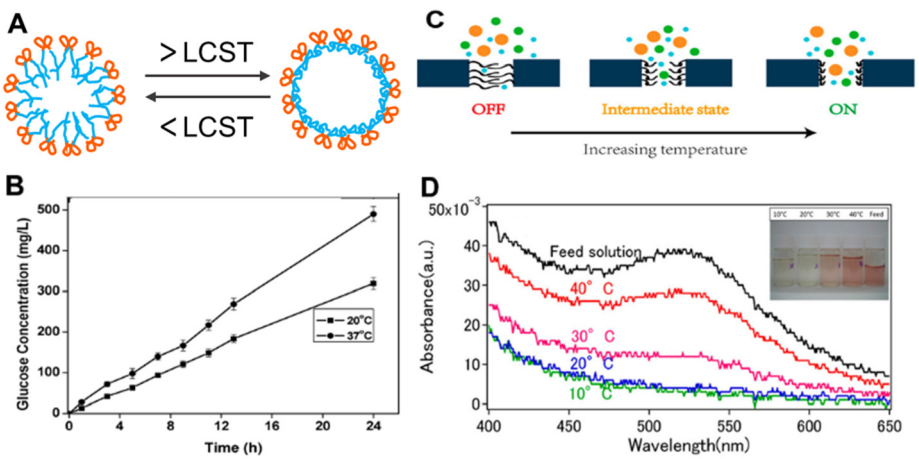

Fig. 12 (A) Schematic depiction of the switchable pore of the thermo-responsive PCL-PNP membrane. (B) Temperature-dependent typical glucose diffusion through thermo-responsive block copolymer PCL-PNP membranes. (C) Schematic depiction of the switchable barrier properties of the thermo-responsive PMENMA-*b*-PS-*b*-PMENMA membrane. (D) UV-vis spectra of feed solution and filtrate showing the temperature-dependent filtration of 5 nm gold colloidal particles using thermo-responsive PMENMA-*b*-PS-*b*-PMENMA membranes. (B) Reprinted with permission from ref. 54. Copyright 2008 American Chemical Society. (C and D) Reprinted with permission from ref. 34. Copyright 2016 American Chemical Society.

3. Conclusions

Thermo-responsive block copolymers are of great interest because of their mature synthesis technology, well-defined structure, controllable molecular weight and easy implementation of temperature regulation. These thermo-responsive block copolymers also have the following advantages: (1) various nano-assemblies with different morphologies, such as spheres, vesicles and petals, can be prepared, allowing the desired structure to meet the requirements; (2) the phase transition of the thermo-responsive block is reversible, which provides great convenience for their material cycling or structure and/or character tuning; (3) most thermo-responsive block copolymers can be applied in aqueous solution, reducing the use of organic solvents and being more friendly to the environment. However, despite all the advantages of thermo-responsive block copolymers, their applications are just at the laboratory research stage. In comparison with polymers synthesized with general radical polymerization, thermo-responsive block copolymers with narrow molecular weight distribution and well-defined block structure are not easy to achieve in large-scale production, which limits their utilization in industry.

In order to bring thermo-responsive block copolymers into large-scale application, efforts should be made in the following areas. First, develop thermo-response originated monomers that can be easily synthesized in large quantities, thereby reducing material cost. Second, improve the long-term durability of thermo-responsive block copolymer materials (*e.g.*, thermal responsive membranes), such as introducing crosslinked structures or interpenetrating networks to improve their mechanical properties. Third, large-scale and controlled approaches for the synthesis of thermo-responsive block copolymers should be further explored.

Author contributions

The manuscript was written through contributions of all authors. All authors have given approval to the final version of the manuscript.

Conflicts of interest

There are no conflicts to declare.

Acknowledgements

The financial support by the Ministry of Science and Technology of the People's Republic of China (2021YFB2500300), the National Science Foundation of China (No. 21931003) and Beijing Nova Program of Science and Technology (Z191100001119122) is gratefully acknowledged.

References

1 X. Chang, C. Wang, G. Shan, Y. Bao and P. Pan, *Langmuir*, 2020, **36**, 956–965.
2 M. Fedorczyk, A. Krzywicka, P. Cieciorski, J. Romanski and E. Megiel, *Polymers*, 2019, **11**, 1484.
3 B. Feher, K. Zhu, B. Nystrom, I. Varga and J. S. Pedersen, *Langmuir*, 2019, **35**, 13614–13623.
4 C. Han, R. Li and Y. Lu, *Energy Fuels*, 2020, **34**, 9473–9482.
5 J. He, J. Cao, Y. Chen, L. Zhang and J. Tan, *ACS Macro Lett.*, 2020, **9**, 533–539.
6 M. Hechenbichler, A. Prause, M. Gradzielski and A. Laschewsky, *Langmuir*, 2022, **38**, 5166–5182.
7 R. Kanto, Y. Qiao, K. Masuko, H. Furusawa, S. Yano, K. Nakabayashi and H. Mori, *Langmuir*, 2019, **35**, 4646–4659.
8 K. Maruya-Li, C. Shetty, A. M. Jazani, N. Arezi and J. K. Oh, *ACS Omega*, 2020, **5**, 3734–3742.
9 H. Zhang, W. Wu, X. Zhao and Y. Zhao, *Macromolecules*, 2017, **50**, 3411–3423.
10 A. Prause, M. Hechenbichler, B. von Lospichl, A. Feoktystov, R. Schweins, N. Mahmoudi, A. Laschewsky and M. Gradzielski, *Macromolecules*, 2022, **55**, 5849–5863.
11 A. Vagias, A. Papagiannopoulos, L. P. Kreuzer, D. Giaouzi, S. Busch, S. Pispas and P. Muller-Buschbaum, *Macromolecules*, 2021, **54**, 7298–7313.
12 I. A. van Hees, P. J. M. Swinkels, R. G. Fokkink, A. H. Velders, I. K. Voets, J. van der Gucht and M. Kamperman, *Polym. Chem.*, 2019, **10**, 3127–3134.
13 M. Cao, H. Nie, Y. Hou, G. Han and W. Zhang, *Polym. Chem.*, 2019, **10**, 403–411.
14 I. R. Dorsman, M. J. Derry, V. J. Cunningham, S. L. Brown, C. N. Williams and S. P. Armes, *Polym. Chem.*, 2021, **12**, 1224–1235.
15 X. Jiang, C. Feng, G. Lu and X. Huang, *ACS Macro Lett.*, 2014, **3**, 1121–1125.
16 X. Jiang, C. Feng, G. Lu and X. Huang, *Polymer*, 2015, **64**, 268–276.
17 M. Cetintas, J. de Grooth, A. H. Hofman, H. M. van der Kooij, K. Loos, W. M. de Vos and M. Kamperman, *Polym. Chem.*, 2017, **8**, 2235–2243.
18 F. Algarni, V. E. Musteata, G. Falca, S. Chisca, N. Hadjichristidis and S. P. Nunes, *Macromolecules*, 2021, **54**, 10235–10250.
19 H. Yoshimitsu, E. Korchagina, A. Kanazawa, S. Kanaoka, F. M. Winnik and S. Aoshima, *Polym. Chem.*, 2016, **7**, 2062–2068.
20 S. Chen, K. Wang and W. Zhang, *Polym. Chem.*, 2017, **8**, 3090–3101.
21 V. Hildebrand, M. Heydenreich, A. Laschewsky, H. M. Möller, P. Müller-Buschbaum, C. M. Papadakis, D. Schanzenbach and E. Wischerhoff, *Polymer*, 2017, **122**, 347–357.
22 N. S. Vishnevetskaya, V. Hildebrand, B. J. Niebuur, I. Grillo, S. K. Filippov, A. Laschewsky, P. Müller-Buschbaum and C. M. Papadakis, *Macromolecules*, 2017, **50**, 3985–3999.

23 H. Yuan, H. Chi and W. Yuan, *Polym. Chem.*, 2016, **7**, 4901–4911.
24 L. P. Kreuzer, T. Widmann, N. Aldosari, L. Bießmann, G. Mangiapia, V. Hildebrand, A. Laschewsky, C. M. Papadakis and P. Müller-Buschbaum, *Macromolecules*, 2020, **53**, 9108–9121.
25 N. S. Vishnevetskaya, V. Hildebrand, B.-J. Niebuur, I. Grillo, S. K. Filippov, A. Laschewsky, P. Müller-Buschbaum and C. M. Papadakis, *Macromolecules*, 2016, **49**, 6655–6668.
26 J. Y. Quek, Y. Zhu, P. J. Roth, T. P. Davis and A. B. Lowe, *Macromolecules*, 2013, **46**, 7290–7302.
27 L. Mäkinen, D. Varadharajan, H. Tenhu and S. Hietala, *Macromolecules*, 2016, **49**, 986–993.
28 N. J. B. C. Li, I. Haq, C. Turner and S. P. Armes, *Langmuir*, 2005, **21**, 11026–11033.
29 P. Biais, M. Engel, O. Colombani, T. Nicolai, F. Stoffelbach and J. Rieger, *Polym. Chem.*, 2021, **12**, 1040–1049.
30 L. Despax, J. Fitremann, M. Destarac and S. Harrisson, *Polym. Chem.*, 2016, **7**, 3375–3377.
31 Q. Li, F. Huo, Y. Cui, C. Gao, S. Li and W. Zhang, *J. Polym. Sci., Part A: Polym. Chem.*, 2014, **52**, 2266–2278.
32 B. H. Lessard, E. J. Y. Ling and M. Marić, *Macromolecules*, 2012, **45**, 1879–1891.
33 Q. Li, C. Gao, S. Li, F. Huo and W. Zhang, *Polym. Chem.*, 2014, **5**, 2961–2972.
34 Y. Tang, K. Ito, L. Hong, T. Ishizone and H. Yokoyama, *Macromolecules*, 2016, **49**, 7886–7896.
35 J. Wu, W. Zhai, X. Gao, B. Liu, R. Zhang and Y. Yu, *Polym. Bull.*, 2020, **78**, 753–768.
36 N. Suzuki, T. Takabe, Y. Yamauchi, S. Koyama, R. Koike, M. Rikukawa, W.-T. Liao, W.-S. Peng and F.-Y. Tsai, *Tetrahedron*, 2019, **75**, 1351–1358.
37 N. Suzuki, S. Koyama, R. Koike, N. Ebara, R. Arai, Y. Takeoka, M. Rikukawa and F. Y. Tsai, *Polymer*, 2021, **13**, 2717.
38 K. Zheng, S. Chen, H. Zhan, J. Situ, Z. Chen, X. Wang, D. Zhang and L. Zhang, *Polymer*, 2022, **260**, 125383.
39 D. Li, J. R. Dunlap and B. Zhao, *Langmuir*, 2008, **24**, 5911–5918.
40 D. Li and B. Zhao, *Langmuir*, 2007, **23**, 2208–2217.
41 H. Jia, R. Roa, S. Angioletti-Uberti, K. Henzler, A. Ott, X. Lin, J. Möser, Z. Kochovski, A. Schnegg, J. Dzubiella, M. Ballauff and Y. Lu, *J. Mater. Chem. A*, 2016, **4**, 9677–9684.
42 K. Nishimori, M. Maruyama, Y. Shimazaki, M. Ouchi and H. Yoshida, *ACS Appl. Polym. Mater.*, 2019, **1**, 1925–1929.
43 J. H. Joe, J. M. Park, H. Lee and W.-D. Jang, *Eur. Polym. J.*, 2019, **118**, 320–326.
44 A. Ferrández-Montero, I. Quijada-Garrido, M. Liras and O. García, *Eur. Polym. J.*, 2016, **84**, 565–576.
45 N. Hu, L. Mi, E. Metwalli, L. Biessmann, C. Herold, R. Cubitt, Q. Zhong and P. Muller-Buschbaum, *Langmuir*, 2022, **38**, 8094–8103.
46 X. Hu, Y. Li, T. Liu, G. Zhang and S. Liu, *ACS Appl. Mater. Interfaces*, 2015, **7**, 15551–15560.
47 Y. S. Chen, S. J. Yoon, W. Frey, M. Dockery and S. Emelianov, *Nat. Commun.*, 2017, **8**, 15782.
48 H. Wang and A. Ullah, *Polymer*, 2022, **14**, 3436.
49 C. R. Becer, K. Kokado, C. Weber, A. Can, Y. Chujo and U. S. Schubert, *J. Polym. Sci., Part A: Polym. Chem.*, 2010, **48**, 1278–1286.
50 P. De and B. S. Sumerlin, *Macromol. Chem. Phys.*, 2013, **214**, 272–279.
51 J. Wu, X. Sun, R. Zhang, S. Yuan, Z. Wu, Q. Lu and Y. Yu, *Colloid Polym. Sci.*, 2016, **294**, 1989–1995.
52 F. Alsubaie, E. Liarou, V. Nikolaou, P. Wilson and D. M. Haddleton, *Eur. Polym. J.*, 2019, **114**, 326–331.
53 J. W. Woodcock, R. A. E. Wright, X. Jiang, T. G. O'Lenick and B. Zhao, *Soft Matter*, 2010, **6**, 3325–3336.
54 F. J. Xu, J. Li, S. J. Yuan, Z. X. Zhang, E. T. Kang and K. G. Neoh, *Biomacromolecules*, 2008, **9**, 331–339.
55 P. Pahl, C. Schwarzenböck, F. A. D. Herz, B. S. Soller, C. Jandl and B. Rieger, *Macromolecules*, 2017, **50**, 6569–6576.
56 A. P. Constantinou and T. K. Georgiou, *Polym. Chem.*, 2016, **7**, 2045–2056.
57 M. Le Bohec, M. Banère, S. Piogé, S. Pascual, L. Benyahia and L. Fontaine, *Polym. Chem.*, 2016, **7**, 6834–6842.
58 M. V. G. Paixão, R. C. S. da Luz and and R. d. C. Balaban, *J. Mol. Liq.*, 2019, **286**, 110792.
59 I. Koonar, C. Zhou, M. A. Hillmyer, T. P. Lodge and R. A. Siegel, *Langmuir*, 2012, **28**, 17785–17794.
60 Y. Hu, V. Darcos, S. Monge, S. Li, Y. Zhou and F. Su, *J. Mater. Chem. B*, 2014, **2**, 2738–2748.
61 B. Hu, W. Fu and B. Zhao, *Macromolecules*, 2016, **49**, 5502–5513.
62 A. Prause, M. Hechenbichler, B. von Lospichl, A. Feoktystov, R. Schweins, N. Mahmoudi, A. Laschewsky and M. Gradzielski, *Macromolecules*, 2022, **55**, 5849–5863.
63 J. Wang, P. Gao, L. Ye, A. Zhang and Z. Feng, *Polym. Chem.*, 2011, **2**, 931–940.
64 M. F. T. Meier, F. Thetiot, N. Pittala, I. Lieberwirth, C. Kunzler, S. Triki and U. Jonas, *Polym. Chem.*, 2021, **12**, 5598–5612.
65 R. Keogh, L. D. Blackman, J. C. Foster, S. Varlas and R. K. O'Reilly, *Macromol. Rapid Commun.*, 2020, **41**, 1900599.
66 M. P. J. Miclotte, S. Varlas, C. D. Reynolds, B. Rashid, E. Chapman and R. K. O'Reilly, *ACS Appl. Mater. Interfaces*, 2022, **14**, 54182–54193.
67 G. Wang, M. Chen, S. Guo and A. Hu, *J. Polym. Sci., Part A: Polym. Chem.*, 2014, **52**, 2684–2691.
68 D. d. M. Zanata and M. I. Felisberti, *Polym. Chem.*, 2021, **12**, 4668–4679.
69 E. Dalgakiran and H. Tatlipinar, *J. Phys. Chem. B*, 2019, **123**, 1283–1293.
70 S. H. Min, S. K. Kwak and B.-S. Kim, *Polymer*, 2017, **124**, 219–225.
71 X. Cai, L. Zhong, Y. Su, S. Lin and X. He, *Polym. Chem.*, 2015, **6**, 3875–3884.
72 X. An, Q. Tang, W. Zhu, K. Zhang and Y. Zhao, *Macromol. Rapid Commun.*, 2016, **37**, 980–986.

73 J. Huang, H. Qin, B. Wang, Q. Tan and J. Lu, *Polym. Chem.*, 2019, **10**, 6379–6384.
74 B. D. Monnery and R. Hoogenboom, *Polym. Chem.*, 2019, **10**, 3480–3487.
75 S. Wiedmann, M. Luitz, B. Kerscher, J.-F. Lutz and R. Mülhaupt, *Macromolecules*, 2019, **52**, 9672–9681.
76 F. Doberenz, K. Zeng, C. Willems, K. Zhang and T. Groth, *J. Mater. Chem. B*, 2020, **8**, 607–628.
77 K. Nagase, A. Ota, T. Hirotani, S. Yamada, A. M. Akimoto and H. Kanazawa, *Macromol. Rapid Commun.*, 2020, **41**, 2000308.
78 E. M. Lewoczko, N. Wang, C. E. Lundberg, M. T. Kelly, E. W. Kent, T. Wu, M.-L. Chen, J.-H. Wang and B. Zhao, *ACS Appl. Polym. Mater.*, 2020, **3**, 867–878.
79 P. A. Woodfield, Y. Zhu, Y. Pei and P. J. Roth, *Macromolecules*, 2014, **47**, 750–762.
80 F. Liu, J. Seuring and S. Agarwal, *J. Polym. Sci., Part A: Polym. Chem.*, 2012, **50**, 4920–4928.
81 M. Pu and M. Hara, *Polymer*, 2014, **55**, 4890–4898.
82 S. L. Perry, L. Leon, K. Q. Hoffmann, M. J. Kade, D. Priftis, K. A. Black, D. Wong, R. A. Klein, C. F. Pierce, K. O. Margossian, J. K. Whitmer, J. Qin, J. J. de Pablo and M. Tirrell, *Nat. Commun.*, 2015, **6**, 6052.
83 B. K. Lee, J. H. Noh, J. H. Park, S. H. Park, J. H. Kim, S. H. Oh and M. S. Kim, *Tissue Eng. Regener. Med.*, 2018, **15**, 393–402.
84 G. Gotzamanis and C. Tsitsilianis, *Polymer*, 2007, **48**, 6226–6233.
85 G. Pasparakis and C. Tsitsilianis, *Polymer*, 2020, **211**, 123146.
86 A. P. Constantinou and T. K. Georgiou, *Eur. Polym. J.*, 2016, **78**, 366–375.
87 Q. Zhang, L. Voorhaar, S. K. Filippov, B. F. Yesil and R. Hoogenboom, *J. Phys. Chem. B*, 2016, **120**, 4635–4643.
88 S. Qiao, M. Mamuti, H. An and H. Wang, *Prog. Polym. Sci.*, 2022, **131**, 101578.
89 K. Nagase, N. Kojima, M. Goto, T. Akaike and H. Kanazawa, *J. Mater. Chem. B*, 2022, **10**, 8629–8641.
90 N. Majstorović, J. Pechtold and S. Agarwal, *ACS Appl. Polym. Mater.*, 2022, **4**, 5395–5403.
91 S. H. Kim, J. P. Tan, K. Fukushima, F. Nederberg, Y. Y. Yang, R. M. Waymouth and J. L. Hedrick, *Biomaterials*, 2011, **32**, 5505–5514.
92 K. Nagase, G. Edatsune, Y. Nagata, J. Matsuda, D. Ichikawa, S. Yamada, Y. Hattori and H. Kanazawa, *Biomater. Sci.*, 2021, **9**, 7054–7064.
93 C. Song, S. Yu, C. Liu, Y. Deng, Y. Xu, X. Chen and L. Dai, *Mater. Sci. Eng., C*, 2016, **62**, 45–52.
94 Z. Iatridi, M. M. S. Lencina and C. Tsitsilianis, *Polym. Chem.*, 2015, **6**, 3942–3955.
95 W. Xu, P. A. Ledin, Z. Iatridi, C. Tsitsilianis and V. V. Tsukruk, *Macromolecules*, 2015, **48**, 3344–3353.
96 F. L. Dévédec, S. Strandman, W. E. Baille and X. X. Zhu, *Polymer*, 2013, **54**, 3898–3903.
97 S. So and T. P. Lodge, *Langmuir*, 2015, **31**, 594–601.
98 J. M. Horton, Z. Bai, X. Jiang, D. Li, T. P. Lodge and B. Zhao, *Langmuir*, 2011, **27**, 2019–2027.
99 M. T. Popescu, D. Tasis and C. Tsitsilianis, *ACS Macro Lett.*, 2014, **3**, 981–984.
100 S. So, L. J. Yao and T. P. Lodge, *J. Phys. Chem. B*, 2015, **119**, 15054–15062.
101 H. Sun, X. Chen, X. Han and H. Liu, *Langmuir*, 2017, **33**, 2646–2654.
102 S. A. Angelopoulos and C. Tsitsilianis, *Macromol. Chem. Phys.*, 2006, **207**, 2188–2194.
103 C. Tsitsilianis, G. Serras, C.-H. Ko, F. Jung, C. M. Papadakis, M. R. Kalourkoti, C. S. Patrickios, R. Schweins and C. Chassenieux, *Macromolecules*, 2018, **51**, 2169–2179.
104 M. M. S. Lencina, C.-H. Ko, F. A. Jung, R. Schweins, M. R. Kalourkoti, C. S. Patrickios, C. M. Papadakis and C. Tsitsilianis, *ACS Appl. Polym. Mater.*, 2021, **3**, 819–829.
105 Q. Li, L. Li, W. Wang, X. Zhang, S. Li, Q. Tian and J. Liu, *RSC Adv.*, 2016, **6**, 45305–45314.